Two-dimensional solidification and melting in potential flows

By LINDA M. CUMMINGS[1], YURI E. HOHLOV[2], SAM D. HOWISON[1] AND KONSTANTIN KORNEV[3]

[1] Mathematical Institute, Oxford University, 24–29 St Giles, Oxford, OX1 3LB, UK

[2] Steklov Mathematical Institute RAS, 42, Vavilova St., 117966 Moscow, Russia

[3] Institute for Problems in Mechanics RAS, 101, prosp. Vernadskogo, 117526 Moscow, Russia

The problem of solidification or melting under the action of a forced hydrodynamic flow is considered. In the appropriate parameter régime, the problem admits a formulation in terms of analytic functions. It is shown that a crystal with a parabolic tip propagates without change of shape at a steady velocity. Some novel explicit solutions are presented.

1. Introduction

The problem of pattern formation in two-dimensional free boundary problems has received much attention; see for example Bensimon *et al.* (1986), Langer (1986), Kessler, Koplik & Levine (1988), Brener & Melnikov (1991), Howison (1992). One such problem is that of dendritic crystallization in the diffusion-limited régime, when the growth velocity is determined by the rate of diffusion of latent heat away from the front (Langer 1986; Kessler *et al.* 1988; Brener & Melnikov 1991). As was first shown by Ivantsov (1947), a dendrite of parabolic shape propagates into a uniform temperature field at a constant velocity; however, the tip radius l and velocity v cannot be selected uniquely within the framework of Ivantsov's approach. In experiments the existence of hydrodynamic flow can play a significant role in the selection process and very little is known about the action of imposed flow on crystal growth. Bouissou, Perrin & Tabeling (1989) considered the influence of hydrodynamic forced flow on the growth process, because the results for this problem help one to understand the selection problem better. Recent theoretical studies (Benamar, Bouissou & Pelce 1988; Dash & Gill 1984; Ananth & Gill 1989, 1991; Xu 1993) have been performed to extend the Ivantsov parabolic solution to potential and viscous flows. In particular, it has been found that the full Navier–Stokes model does not have an exact similarity solution for forced convection (Ananth & Gill 1989, 1991; Xu 1993); there is however an exact solution when the flow is driven by a density change at the interface (Howison 1988). On the other hand, solidification/melting in the presence of a potential flow *does* admit an Ivantsov-like solution (Benamar *et al.* 1988; Dash & Gill 1984).

Such problems arise, for example, in the context of models of artificial freezing and thawing of flows in porous media (Maksimov 1965, 1976; Goldstein & Reid 1978; Kornev & Mukhamadullina 1994) assuming that pore size within the medium is small relative to the size of the frozen body, and are applicable to the study of crystal solidification and melting in a Hele-Shaw cell. In fact, the behaviour of our solutions bears a close resemblance to solutions of the one-phase zero-surface-tension

$$\frac{\partial \theta}{\partial y} \longrightarrow 0$$

$$\nabla \cdot \boldsymbol{V} = 0, \qquad \boldsymbol{V} = \nabla \varphi$$

$$Pe\, \boldsymbol{V} \cdot \nabla \theta = \nabla^2 \theta$$

$$\boldsymbol{V} \longrightarrow \boldsymbol{V}_\infty$$
$$\theta \longrightarrow \theta_\infty$$

Liquid

Dendrite

$\Omega(t)$

$\theta = 0$

$$\frac{\partial \theta}{\partial n} = -v_n$$
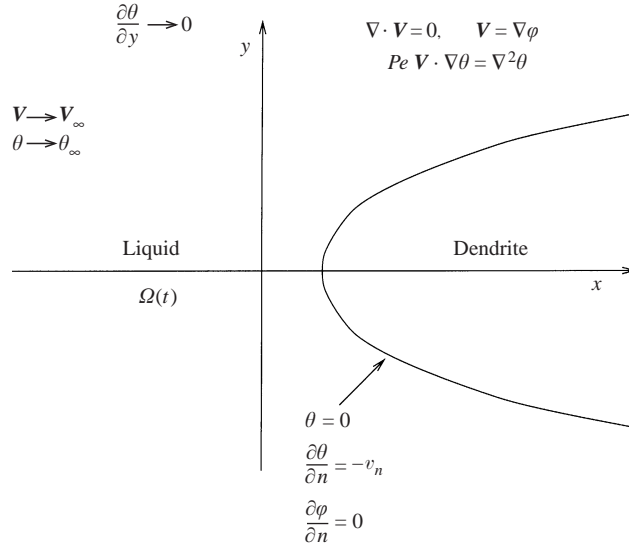
$$\frac{\partial \varphi}{\partial n} = 0$$

FIGURE 1. Schematic diagram of the geometry (in the dimensionless variables).

Hele-Shaw problem, melting being analogous to the stable case where fluid is injected into the cell, and crystallization to the unstable suction case, and we return to this analogy later. However, it should be noted that crystallization in a rectangular cell or capillary, and solidification of a binary system or a pure material, may radically change the selection principle. Bouissou *et al.* (1989) consider a binary system in a rectangular cell, while other theoretical studies (Ananth & Gill 1989, 1991; Benamar & Pelce 1988; Dash & Gill 1984; Xu 1993) operate with flows of pure melt. As experimentally shown by Lee, Ananth & Gill (1993), the results for a pure material solidifying within a cylindrical capillary are opposite to those of Bouissou *et al.* (1989), so the theoretical treatment of existing experimental data should be approached with caution.

Briefly, the layout of this paper is as follows: we first formulate the problem of quasistatic two-dimensional solidification and melting in potential flows in terms of analytic functions. Such a formulation allows us to calculate more complicated evolution than simple travelling waves, and enables us to show a relationship between solidification problems and the purely hydrodynamical Hele-Shaw flow. Semi-infinite frozen bodies will be considered, and as examples, the steady growth of a parabolic dendrite, a flat interface, and the unsteady growth of irregularities which we call 'cracks' will be discussed.

2. Mathematical model

We consider a situation in which part of a saturated porous medium is frozen, at the melting temperature T_m (assumed constant), while in the remainder the unfrozen liquid flows according to Darcy's law (see figure 1 for a sketch). The unfrozen liquid flows from left to right, and the frozen region grows from the right. We assume that the liquid is incompressible, and that the thermophysical parameters of the matter are constant. The temperature and the velocity at infinity are denoted by T_∞ and V_∞ respectively. The former is taken to be constant, while the latter represents a far-field flow and may vary spatially. In the case $T_\infty > T_m$ the frozen region recedes,

and solutions describe a melting dendrite in a warm flow, and when $T_\infty < T_m$ we have the opposite situation of a dendrite growing into an oncoming supercooled liquid.

In the dendrite cross-section we introduce the coordinate system $z = x + \mathrm{i}y$ and the complex flow potential $W = \varphi + \mathrm{i}\psi$, where φ is the velocity potential and ψ is the stream function. The variables x, y and function W are dimensionless, so $\hat{x} = lx$, $\hat{y} = ly$ and $\hat{W} = V_\infty l W$ where the hatted variables are dimensional, and l is a characteristic dendrite size, which must be determined. The velocity potential is related to the pressure p by $\varphi = -kp/(V_\infty \mu l)$ where k is the permeability of the medium and μ is the viscosity of the fluid. Gravity is neglected. The mathematical model in the dimensionless variables then has the form

$$
\left.
\begin{aligned}
\nabla \cdot \boldsymbol{V} = 0, \qquad \boldsymbol{V} = \nabla \varphi, \qquad Pe\, \boldsymbol{V} \cdot \nabla \theta = \nabla^2 \theta, \qquad z \in \Omega(t); \\[2mm]
\theta = 0, \qquad -\frac{\partial \theta}{\partial n} = v_n, \qquad \frac{\partial \varphi}{\partial n} = 0, \qquad z \in \partial\Omega(t); \\[2mm]
\boldsymbol{V} \to \boldsymbol{V}_\infty \quad \text{as } |z| \to \infty; \\[2mm]
\lim_{x \to -\infty} \theta = \theta_\infty, \quad \lim_{y \to \pm\infty} \frac{\partial \theta}{\partial y} = 0; \\[2mm]
\Omega(t)\big|_{t=0} = \Omega_0.
\end{aligned}
\right\}
\tag{2.1}
$$

Here v_n is the normal (outward with respect to the liquid region) velocity of dendrite growth, in which time has been made dimensionless with the thermal time $l^2 \rho L / (\kappa |T_\infty - T_m|)$; L is the latent heat, and κ is the thermal conductivity of the liquid. The function $\theta = (T - T_m)/|T_\infty - T_m|$ describes the temperature field within the liquid; with this normalization the two possibilities we consider are $\theta_\infty = \pm 1$ (melting, and crystallization with supercooling, respectively). The Péclet number $Pe = V_\infty l / D$ is a measure of the intensity of heat transfer by convection compared with conduction, and D is the thermal diffusivity of the liquid. The region Ω is occupied by liquid, $\partial\Omega$ is its boundary, and Ω_0 is the corresponding initial domain.

In fact we only need consider one of the two problems (melting or crystallization), since reversing the sign of the temperature ($\theta \mapsto -\theta$) leaves the model unchanged apart from the kinematic boundary condition and the condition on θ at infinity, which are both reversed. Hence, if we can obtain the free boundary evolution of, say, a melting dendrite using the model (2.1) with $\theta_\infty = 1$, reversing time in this evolution describes a solid dendrite *growing* in a supercooled liquid. We shall assume this 'time-reversibility' freely in our solutions.

Note that we have assumed a quasi-static model for the heat flow, which is why the normal velocity in the Stefan condition '$-\partial\theta/\partial n = v_n$ on $\partial\Omega$' has been scaled using the timescale $l^2 \rho L / (\kappa |T_\infty - T_m|)$ instead of with V_∞. This model is therefore applicable to the common situation in which the volume heat capacity is negligible compared with the latent heat (Goldstein & Reid 1978; Glicksman, Coriell & McFadden 1986). We also assume that the imposed hydrodynamic velocity is much greater than the velocity caused by the solid–liquid density difference, and the stronger condition that the velocity of the forced flow is much greater than the velocity of crystallization (we comment briefly on this assumption in the Conclusions). Then the frozen body at any instant of time serves as a quasi-static obstacle for the flow; this is why the boundary condition for the potential does not involve v_n. When hydrodynamic and crystallization velocities are comparable the problem is more complicated and we cannot directly apply the technique proposed below. However, the experimental
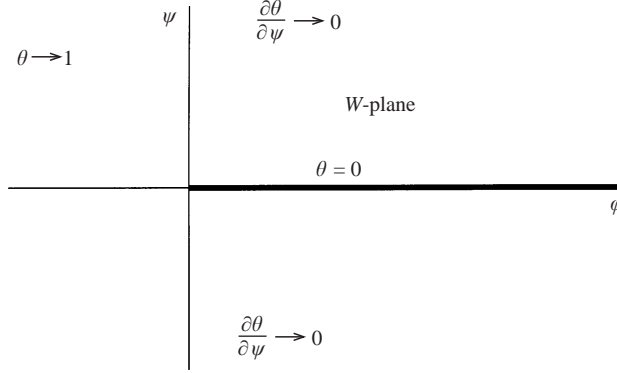
FIGURE 2. Diagram of the problem in the Boussinesq plane.

situation described above is widespread (Bouissou *et al.* 1989; Goldstein & Reid 1978), and the model is reasonable.

3. Uncoupling of the problem

It is remarkable that the moving boundary problem (2.1) may be split into two independent subtasks (Maksimov 1965, 1976; Goldstein & Reid 1978; Kornev & Mukhamadullina 1994), the first of which is the problem of heat exchange between a semi-infinite isothermal knife and a homogeneous flow. The second subtask contains all the 'free boundary' aspects of the problem. The split is effected by applying the Boussinesq transformation (Boussinesq 1905) to the convective heat transfer equation, which is equivalent to a conformal mapping from the liquid region in the physical plane onto a domain in the complex potential (W) plane, or using φ, ψ as independent variables. The equation for the temperature field θ remains invariant under this transformation, and is

$$Pe\,\frac{\partial \theta}{\partial \varphi} = \frac{\partial^2 \theta}{\partial \varphi^2} + \frac{\partial^2 \theta}{\partial \psi^2}. \tag{3.1}$$

The body cross-section maps into the cut directed along the positive real axis $\psi = 0$, $\varphi > 0$ in the complex potential W-plane (figure 2). In accordance with the above we have

$$\lim_{\varphi \to -\infty} \theta = 1, \quad \lim_{\psi \to \pm\infty} \frac{\partial \theta}{\partial \psi} = 0; \qquad \theta = 0 \quad \text{on } \varphi \in [0, \infty), \quad \psi = \pm 0. \tag{3.2}$$

Introducing the further transformation $(\psi, \varphi) \mapsto (\xi, \eta)$, given in complex form by

$$W = \omega^2, \qquad \omega = \xi + i\eta,$$

(in the complex variable interpretation we have mapped from the cut W-plane to the upper-half ω-plane) we look for a similarity solution $\theta = f(\eta)$.† This leads to the ordinary differential equation and boundary conditions

$$f''(\eta) + 2Pe\,\eta\,f'(\eta) = 0 \quad (\eta > 0), \qquad f(0) = 0, \quad f(\infty) = 1,$$

† There are several possible ways of deriving the resulting temperature field; see for instance Benamar *et al.* (1988), Dash & Gill (1984), Wijngaarden (1966).

and the explicit solution is then easily obtained as

$$\theta = f(\eta) = 2\left(\frac{Pe}{\pi}\right)^{1/2}\int_0^{\eta}\exp(-Pe\,s^2)\,\mathrm{d}s. \tag{3.3}$$

We remark here that the 'backward problem', in which the flow direction is reversed, is much more difficult. The Péclet number changes sign in the dimensionless model, corresponding to heat being convected in the opposite direction, and we cannot expect to be able to impose the same boundary conditions at infinity (it is easily checked that there is no similarity solution of the kind proposed above). We must specify conditions upstream, not down, but which conditions? This $Pe < 0$ problem is essentially the (local) rear stagnation-point problem for flow past a finite body, whereas the $Pe > 0$ problem is the (local) forward stagnation-point problem, which is much simpler. To solve for the rear problem we must solve (i) the forward problem; (ii) the outer problem (matching onto the solution of (i)); and finally, the rear problem, matching onto (ii). We do not consider such complications in this paper.

An alternative method of solution is given by Wijngaarden (1966): by using the Green's function for the Helmholtz equation, the problem (3.1)–(3.2) can be reduced to the integral equation

$$\pi = \int_0^{\infty}\frac{\partial\theta}{\partial\psi}\,\exp\left(\frac{Pe}{2}(\varphi - \xi)\right)K_0\left(\frac{Pe}{2}|\varphi - \xi|\right)\mathrm{d}\xi,$$

where $K_0(z)$ is the modified Bessel function. This integral equation can be solved in closed form using the Wiener–Hopf technique.

It is easily seen from the solution (3.3) (and it can be deduced from the integral equation formulation above) that on the cut $\psi = 0$,

$$\left|\frac{\partial\theta}{\partial\psi}\right| = \left(\frac{Pe}{\pi\varphi}\right)^{1/2}. \tag{3.4}$$

The combination $(Pe/\pi)^{1/2}$ arises many times in the following, so henceforth we write $\sigma = (Pe/\pi)^{1/2}$.

Using the relation (3.4), the heat flux at the unknown boundary is transformed to

$$\left|\frac{\partial\theta}{\partial n}\right| = \left|\frac{\partial\theta}{\partial\psi}\right|\left|\frac{\partial\psi}{\partial n}\right| = \left|\frac{\partial\theta}{\partial\psi}\right|\left|\frac{\partial W}{\partial z}\right| = \frac{\sigma}{\varphi^{1/2}}\left|\frac{\partial W}{\partial z}\right|. \tag{3.5}$$

This condition enables us to reformulate the initial problem in terms of analytic functions, just as for the Hele-Shaw problem (Bensimon *et al.* 1986; Kessler *et al.* 1988; Howison 1992).

4. The Polubarinova–Galin equation

We again consider the auxiliary plane $\omega = \xi + i\eta$ (the plane of canonical variables) so that the upper half of the plane corresponds to the flow region, recalling that $W = \omega^2$. We take the origin at the stagnation point and the corresponding point in the auxiliary plane is also placed at $\omega = 0$. Let the function f map the upper half of the ω-plane onto the region $\Omega(t): z = f(\omega, t)$. The unit vector normal to the moving interface $\partial\Omega(t) = x_0(t) + iy_0(t)$ can be expressed as

$$\boldsymbol{n} = n_x + \mathrm{i}n_y = \mathrm{i}\frac{\partial f}{\partial\omega}\left|\frac{\partial f}{\partial\omega}\right|^{-1},$$

on the boundary $\omega = \xi$. The normal velocity of the interface then has the form

$$v_n = (\dot{x}_0 n_x + \dot{y}_0 n_y) = \text{Re}\left\{(\dot{x}_0 + i\dot{y}_0)(n_x - in_y)\right\}$$

$$= \text{Re}\left\{\frac{\partial f}{\partial t}\overline{i\frac{\partial f}{\partial \omega}}\left|\frac{\partial f}{\partial \omega}\right|^{-1}\right\}, \qquad \xi \in (-\infty, \infty), \quad \eta \to +0. \tag{4.1}$$

On the other hand, the boundary of the frozen region is a streamline, so at the dendrite interface we have

$$\pm i\left|\frac{\partial \theta}{\partial \psi}\right|\overline{(V_x - iV_y)} = \pm i\left|\frac{\partial \theta}{\partial \psi}\right|\overline{\frac{\partial W}{\partial z}} = -v_n\boldsymbol{n}, \qquad \psi = \pm 0. \tag{4.2}$$

Combining equations (3.4)–(4.2) we get the condition

$$\text{Re}\left\{\frac{\partial f}{\partial t}\overline{i\frac{\partial f}{\partial \omega}}\right\} = -\frac{\sigma}{W^{1/2}}\overline{\frac{\partial W}{\partial \omega}}, \qquad \xi \in (-\infty, \infty), \quad \eta \to +0. \tag{4.3}$$

In (4.3) we have taken into account the multivalence of the square root, whereby the heat fluxes at different sides of the cut have different signs. Finally using

$$W = \omega^2, \tag{4.4}$$

we obtain the Polubarinova–Galin (P-G) equation (Howison 1992)

$$\text{Re}\left\{\frac{\partial f}{\partial t}\overline{i\frac{\partial f}{\partial \omega}}\right\} = -2\sigma, \qquad \xi \in (-\infty, \infty), \eta = 0. \tag{4.5}$$

(This same equation arises in the zero-surface-tension Hele-Shaw problem with an imposed pressure gradient; see for instance Howison 1992.) In the dimensional variables the factor of 2σ on the right-hand side of (4.5) becomes $2L\rho V_\infty l/(\kappa|T_\infty - T_m|(\pi D)^{1/2})$.

In addition to the boundary condition (4.5), we must specify the asymptotic behaviour of the function f at infinity, and the initial dendrite shape. For the former, we can use the boundary condition for the velocity at infinity. We specify the initial dendrite shape as

$$f(\omega, 0) = f_0(\omega), \tag{4.6}$$

where f_0 is the mapping of the upper half-plane onto the initial region Ω_0. Thus, the boundary value problem (2.1) is reduced to the nonlinear boundary value problem (4.5)–(4.6) for analytic functions f, together with a boundary condition at infinity.

We observe (for later use in § 8) that there is another simple situation which leads to the same P-G equation. Consider an asymptotically-flat semi-infinite solid region, and a flow which is roughly parallel to it, so that in the dimensional variables $\hat{\psi} \to V_\infty \hat{y}$ as $\hat{y} \to \infty$ (in contrast to the oncoming, stagnation-point flow assumed so far). Suppose further that a constant temperature gradient is imposed across the flow, so $\partial T/\partial \hat{y} \to \Delta$ as $\hat{y} \to \infty$ ($\Delta > 0$ gives rise to melting, $\Delta < 0$ to freezing; but again the 'time-reversibility' means that we need only consider $\Delta > 0$).

In the Boussinesq plane the flow domain will be exactly the upper half-plane $\psi \geqslant 0$. Replacing $|T_\infty - T_m|$ by $|\Delta|l$ in the scalings of § 2, the solution for the dimensionless temperature is exactly $\theta = \psi$. This satisfies the boundary condition on $\psi = 0$ and, since (in the dimensionless variables) $\psi \to y$ as $y \to \infty$, does indeed give rise to a constant temperature gradient at infinity in the physical plane. The analogue of equation (3.4) is then $|\partial \theta/\partial \psi| = 1$, and (3.5) becomes $|\partial \theta/\partial n| = |\partial W/\partial z|$. In this geometry the variables ω and W coincide, and following through the argument which

led to (4.5) we find

$$\mathrm{Re}\left\{\frac{\partial f}{\partial t}\mathrm{i}\overline{\frac{\partial f}{\partial \omega}}\right\} = -1, \tag{4.7}$$

which is exactly the same P-G equation (if $\sigma = 1/2$). In the dimensional form of the right-hand side, the factor of 1 is replaced by $\rho L V_\infty^{1/2}/(\kappa|\Delta|l^{1/2})$.

5. Reformulation as an integral equation

Assuming that $z = f(\omega, t)$ is an acceptable parametrization of the moving boundary at least for small t, i.e. that f is a univalent function on the upper half-plane, one can rewrite the condition (4.5) in the form

$$\mathrm{Re}\left\{-\mathrm{i}\frac{\partial f}{\partial t}\Big/\frac{\partial f}{\partial \omega}\right\} = -2\sigma\left|\frac{\partial f}{\partial \omega}\right|^{-2}, \qquad \xi \in (-\infty, \infty), \quad \eta = 0.$$

The application of the Schwarz (Poisson) formula to this condition enables one to determine the analytic function $(\partial f/\partial t)/(\partial f/\partial \omega)$ in the upper half-plane $\eta > 0$ via its real part on the real axis (the boundary of the upper half-plane). One can express condition (4.5) in the form of a nonlinear, non-local partial differential equation for the Riemann mapping function $f(\omega, t)$:

$$\frac{\partial f}{\partial t} = -\frac{\partial f}{\partial \omega}\frac{2\sigma}{\pi}\int_{-\infty}^{\infty}\left|\frac{\partial f}{\partial \zeta}(\zeta, t)\right|^{-2}\frac{\mathrm{d}\zeta}{\zeta - \omega}, \quad \mathrm{Im}(\omega) > 0. \tag{5.1}$$

We call (5.1) a *Löwner–Kufarev type equation* because of the analogy with the well-known linear partial differential equation which appears in univalent function theory (Aleksandrov 1976; Pommerenke 1973). The kinematic condition on the moving boundary $\partial\Omega(t)$ is represented in the form (4.5) for the boundary values of the Riemann mapping function $z = f(\omega, t)$ if and only if the Löwner–Kufarev type equation (5.1) holds for the analytic mapping function $z = f(\omega, t)$ in the upper half-plane. In fact, as well as the above-mentioned conclusion (that equation (5.1) follows from (4.5)), it can be shown conversely that, taking the limit as ω tends to ξ on the real axis, and using the Sokhotsky–Plemelj formulae (Muskhelishvili 1968), the equation (5.1) becomes equivalent to the kinematic condition in the form (4.5). We return to this formulation of the problem in § 8.

6. The Schwarz function

The integro-differential equation (5.1) for the function of time and spatial variable is complicated and can be used only for numerical calculations of the dendritic shape. A useful alternative approach enabling many exact solutions to be constructed is provided by considering the Schwarz function of the free boundary.

We first recall some properties of the Schwarz function (Howison 1992; Davis 1974). It is obtained by substituting for $x = (z + \bar{z})/2$, $y = (z - \bar{z})/2i$ into the equation $F(x, y, t) = 0$, describing the boundary of the dendrite. Solving this equation for $\bar{z}$ in the form

$$\bar{z} = g(z, t), \tag{6.1}$$

we obtain the Schwarz function of $\partial\Omega(t)$ (Howison 1992; Davis 1974). It only exists for

analytic curves in (x, y)-space, and is itself an analytic function in some neighbourhood of the curve. The following relations will be useful:

$$\frac{\mathrm{d}z}{\mathrm{d}s} = \left(\frac{\partial g}{\partial z}\right)^{-1/2}, \tag{6.2}$$

$$v_n = \frac{\mathrm{i}}{2}\frac{\partial g}{\partial t}\left(\frac{\partial g}{\partial z}\right)^{-1/2}; \tag{6.3}$$

hereafter s is arclength and all the formulæ hold for $z \in \partial\Omega$. We can now relate g to the complex potential $W(z, t)$. Because the boundary of the dendrite is a streamline, we have

$$\frac{\mathrm{d}W}{\mathrm{d}z} = \frac{\mathrm{d}W}{\mathrm{d}s}\left(\frac{\mathrm{d}z}{\mathrm{d}s}\right)^{-1} = \left(\frac{\partial g}{\partial z}\right)^{1/2}\frac{\partial \psi}{\partial n}. \tag{6.4}$$

Expressing $\partial\psi/\partial n$ in (6.4) via the heat flux and the normal velocity of the moving boundary (equations (3.5) and (3.4)), and then using (6.3), we arrive at the equation

$$\frac{1}{W^{1/2}}\frac{\mathrm{d}W}{\mathrm{d}z} = -\frac{\mathrm{i}}{2\sigma}\frac{\partial g}{\partial t}. \tag{6.5}$$

Both sides are analytic on $\partial\Omega$ and hence (6.5) holds wherever both functions exist. Equation (6.5) differs from the ordinary Hele-Shaw equations for the Schwarz function given by Richardson (1972), Lacey (1982) and Millar (1989), though the analogy is very close.

We can write $g(z, t)$ in terms of the mapping function $f(\omega, t)$, which allows us to use the above result to construct explicit solutions. By definition, the function $f(\omega, t)$ maps $\eta > 0$ onto $\Omega(t)$ and $\eta = 0$ onto $\partial\Omega(t)$. Then, on the moving boundary, we have $\bar{z} = \overline{f(\omega, t)} = \bar{f}(\bar{\omega}, t) = \bar{f}(\omega, t)$, i.e. the equation

$$g(z, t) = \bar{f}(\omega, t), \tag{6.6}$$

holds on $\partial\Omega$. But since f is analytic on the (closed) upper half-plane, $\bar{f}$ is analytic on the closed lower half-plane, so both sides of this equality are analytic in some neighbourhood of the boundary (considering z as a function of ω, or vice versa). Hence (6.6) may be analytically continued away from the boundary, and holds wherever both sides are defined. It follows that g has singularities in the upper half-plane at the complex conjugates of those of f in the lower half-plane. Hence, since W is analytic in $\eta > 0$ (except possibly at infinity), (6.5) implies that any singularities of the Schwarz function are completely determined by $g(z, 0)$ and must necessarily be constant both in magnitude and in position. The Schwarz function method is well-suited to functions which have poles or logarithmic branch points in the lower half-plane. It offers a basis for the construction of novel classes of explicit non-trivial solutions. We shall demonstrate the efficacy of the statement in terms of analytic functions by giving some simple examples.

7. Ivantsov's dendrite

We first reproduce the Ivantsov solution, i.e. we show that a dendrite of parabolic shape grows at constant velocity. Thus we consider a dendrite whose transverse size increases at infinity not faster than $x^{1/2}$. This solution was obtained by different means by Benamar *et al.* (1988), Dash & Gill (1984).

To obtain such a solution we use the condition for the (dimensionless) flow velocity at infinity given in (2.1), namely

$$\frac{\partial W}{\partial f} = \frac{\partial W}{\partial \omega}\frac{\partial \omega}{\partial f} = 1, \quad \omega \to \infty. \tag{7.1}$$

Equation (7.1) implicitly assumes that the symmetry axis of the dendrite is aligned in the x-direction. Using (4.4) in (7.1), we see that

$$f \sim \omega^2, \quad \omega \to \infty. \tag{7.2}$$

Considering the problem (4.5), (4.6), (7.2) for $f(\omega, t)$, we seek the steady shape of a dendrite growing in supercooled liquid. We postulate the following parabolic ansatz for the solution of this problem:

$$f(\omega, t) = \omega^2 + \mathrm{i}A(t)\omega + B(t), \tag{7.3}$$

with

$$f_0(\omega) = \omega^2 + B(0).$$

Then the condition (7.2) is satisfied automatically and equation (4.5) leads to the formulæ

$$\dot{A} = 0; \quad B = \frac{2\sigma t}{A}. \tag{7.4}$$

Without loss of generality we can take $A = 1$ (this means that all spatial variables are normalized by the tip radius l). As an alternative to using the P-G equation, we can obtain the same solution using the Schwarz function result (6.5) above. The Schwarz function $g(z, t)$ is given by

$$g(z, t) = \overline{f}(\omega, t) = \omega^2 - \mathrm{i}A(t)\omega + B(t),$$

where ω is given as a function of z by inverting (7.3). The left-hand side of equation (6.5) is singular only at infinity, where $W(z) \sim z$ (a simple pole), hence we must find the behaviour of $\partial g/\partial t$ at infinity and match in (6.5). Inversion of the map (7.3) reveals that

$$g(z, t) = z - 2\mathrm{i}Az^{1/2} - A^2 + \frac{\mathrm{i}A}{z^{1/2}}\left(B + \frac{A^2}{4}\right) + O(z^{-3/2}).$$

Equating the behaviours at infinity in (6.5), we retrieve equations (7.4) again.

In dimensional form we find the velocity of propagation of the parabolic dendrite as

$$v = \frac{2\kappa|T_\infty - T_m|}{L}\left(\frac{V_\infty}{\pi l D}\right)^{1/2}. \tag{7.5}$$

Thus, as with Ivantsov's original solution, we have indeterminacy, in that we obtain only a relation between the tip radius and the velocity, and no unique 'selection principle' telling us what both l and v are. As expected (since we consider a different régime) our formula (7.5) differs from Ivantsov's, and we cannot take the limit $V_\infty \to 0$ because the approximation we made in our model is not then valid.† Recall that we assumed the hydrodynamic velocity to be much greater than the crystallization

† We do not present Ivantsov's formula here, since is given in a complicated implicit form which makes a direct comparison difficult.

velocity v, which is what enabled us to separate the Boussinesq problem from the free-boundary problem itself. In the opposite limit in which the crystallization velocity dominates, the explicit solution is more complicated and has been presented by Benamar *et al.* (1988), Dash & Gill (1984). In the latter paper the authors find a dimensionless heat flux (Nusselt number) for the potential flow around the parabolic dendrite, which at the stagnation point has the value $\mathrm{Nu} = (2Pe/\pi)^{1/2}$ (equation (93) of Dash & Gill 1984). In our notation, this equates to a dimensional heat flux at the stagnation point of magnitude

$$\left| \frac{\partial T}{\partial n} \right| = \frac{|T_\infty - T_m|}{l} \left(\frac{2Pe}{\pi} \right)^{1/2}. \tag{7.6}$$

While the Stefan boundary condition that we use is not the appropriate one for their analysis, it is worth remarking that if we naively substitute (7.6) into this condition, we find an 'effective' growth velocity

$$v_e = \frac{\kappa |T_\infty - T_m|}{L} \left(\frac{2V_\infty}{\pi l D} \right)^{1/2},$$

so the result is the same as ours modulo an unimportant constant.†

8. Linear stability of flat interfaces

As a basis for a morphological stability analysis (Mullins & Sekerka 1963, 1964) we examine the growth of a flat interface at constant velocity. The first case we consider is with an extensional-type fluid flow, i.e. a stagnation point flow against a flat interface. Although this seems unlikely at first sight, it is obvious when we note that there is a stagnation point at the tip of a steadily-propagating parabolic dendrite, which is of course locally flat. Indeed, the flat interface solution could be derived by a local expansion of the Ivantsov solution; however, it is simpler to derive it directly.

At infinity the complex potential W has behaviour $W \sim -\alpha z^2/2$, with prescribed velocity gradient α, so the velocity field is $(u, v) \sim (-\alpha x, \alpha y)$. In this case, the boundary condition at infinity is written in dimensional form as

$$\frac{\partial W}{\partial f} = \frac{\partial W}{\partial \omega} \frac{\partial \omega}{\partial f} \sim -\alpha f \quad \text{as } \omega \to \infty. \tag{8.1}$$

The scalings used are those of §2, where the characteristic velocity V_∞ is chosen as $V_\infty = \alpha l$ (the characteristic lengthscale l is introduced for convenience, and does not appear in the resulting formula for the moving interface).

We consider the linear mapping

$$f = i\sqrt{2}\omega + B(t), \tag{8.2}$$

from the upper half-plane to the fluid region (all the parameters are dimensionless). This gives a solution of equation (4.5) provided the parameter $B(t)$ satisfies

$$B(t) = \sqrt{2}\sigma t. \tag{8.3}$$

(This solution is also trivial to obtain using the 'Schwarz function' method.)

We now consider the stability of this interface to small periodic perturbations. It is convenient to do this using the Löwner–Kufarev formulation of equation (5.1).

† The authors are indebted to an anonymous referee for suggesting this comparison.

We assume the same flow conditions at infinity, and expand the mapping function in powers of the small parameter ϵ (which measures the deviation of the interface from the flat) as

$$f(\omega, t) = f^{(0)}(\omega, t) + \epsilon f^{(1)}(\omega, t) + O(\epsilon^2),$$

where $f^{(0)}$ is the solution to the unperturbed problem found above. Substituting into (5.1) gives the $O(\epsilon)$ problem

$$f_t^{(1)} = \frac{2i\sigma}{\pi} \int_{-\infty}^{\infty} \frac{\text{Im}(f_\zeta^{(1)})}{\zeta - \omega} d\zeta - i\sigma f_\omega^{(1)}, \qquad \text{Im}(\omega) > 0 \qquad (8.4)$$

(the subscripts denote partial derivatives). The interface is described by the mapping function $f(\xi, t)$ for $\xi \in (-\infty, \infty)$, thus on the boundary,

$$z = x + iy = i\sqrt{2}\xi + \sigma\sqrt{2}t + \epsilon f^{(1)}(\xi, t). \qquad (8.5)$$

We seek the Fourier modes for the boundary values $f^{(1)}(\xi, t)$ of the form

$$f^{(1)}(\xi, t) = F(k, t)e^{ik\xi};$$

the wavenumber k must be positive to ensure analyticity of $f^{(1)}$ in the upper half-plane. When substituting in (8.4) we need the relation

$$\begin{aligned}
2i \int_{-\infty}^{\infty} \frac{\text{Im}(f_\zeta^{(1)})}{\zeta - \omega} d\zeta &= \int_{-\infty}^{\infty} \frac{f_\zeta^{(1)}(\zeta, t) - \overline{f^{(1)}}_\zeta(\zeta, t)}{\zeta - \omega} d\zeta \\
&= ikF(k, t) \int_{-\infty}^{\infty} \frac{e^{ik\zeta}}{\zeta - \omega} d\zeta + ik\overline{F(k, t)} \int_{-\infty}^{\infty} \frac{e^{-ik\zeta}}{\zeta - \omega} d\zeta \\
&= -2\pi k F(k, t)e^{ik\omega}.
\end{aligned}$$

The last equality is obtained by two separate contour integrals, the first around a large semicircle in the upper half-plane, since this is where $e^{ik\zeta}$ decays, and the second around a semicircle in the lower half-plane, where $e^{-ik\zeta}$ decays. Using this in equation (8.4) then, in the limit $\text{Im}(\omega) \to 0$ we obtain

$$F_t(k, t) = -\sigma k F(k, t).$$

On the boundary (8.5) gives

$$z = x + iy = i\sqrt{2}\xi + \sigma\sqrt{2}t + \epsilon F(k, t)e^{ik\xi}.$$

Thus in the case of melting we have a stable solution, with perturbations decaying exponentially like $\exp(-\lambda t)$, where $\lambda = \sigma k$. (Recalling the scaling used for time, the dimensional dispersion is $\hat{\lambda} = (\alpha/\pi D)^{1/2}(\kappa q|T_\infty - T_m|)/(\rho L)$, where the dimensional wavenumber q is defined by $q = k/l$.) The freezing behaviour is given by the time-reversal of this analysis, hence here we have an *unstable solution*. This analysis should be relevant for the stability of the tip of a steadily-growing dendrite, which as already noted is locally flat.

  The other situation we consider is the stability of a flat interface in a parallel flow, across which a uniform temperature gradient Δ is imposed (this situation was considered at the end of §4). This will be the local situation on the *sides* of a steadily growing dendrite, hence this analysis should indicate the stability in this régime. As observed in §4, although this is a different physical problem it leads to the same P-G equation, and hence the same Löwner–Kufarev formulation (5.1). It follows from this that the basic travelling-wave solution about which we perturb must be given by (8.2)

and (8.3) (with $\sigma = 1/2$), and therefore that the stability analysis carried out above follows through in this case also. Hence we have the same result that melting is stable, and crystallization is unstable, with the dimensionless dispersion relation $\lambda = k/2$. The dimensional relation, showing the dependence on the temperature gradient $\varDelta$, is $\hat{\lambda} = q\kappa|\varDelta|/(2\rho L)$, where again $q = k/l$. The timescales in these two situations differ, due to the different instability mechanisms (though they will be related if we are considering the coupled problems of flow at the nose, and flow around the sides of the dendrite). For the stagnation point flow the forced convection plays an important role, but for the parallel flow the instability is caused solely by the conductivity transport (as in the ordinary Mullins–Sekerka instability (Mullins & Sekerka 1963, 1964)).

Note that the dispersion relations for each case are unbounded, since they increase linearly with the wavenumber q. This is due to the neglect of regularizing surface effects in the analysis; if we included the relevant effects the dispersion relations would be modified, and presumably bounded. However, as we observe later in §10, the precise form of the regularization we should use for the porous medium problem is unclear.

We comment here that Brattkus & Davis (1988) have also considered the effect of forced flow on the stability of a solidifying interface. However, they used the boundary-layer approximation, so their analysis does not apply in the neighbourhood of the stagnation point. In another related work, Davis (1990), the effective decoupling of hydrodynamic disturbances and thermal disturbances is discussed in detail. It is surprising, but to our knowledge nobody has previously studied the stability of the interface for forced potential flow at the stagnation point.

9. Unsteady solutions

We turn now to exact unsteady solutions. As mentioned in §6, a novel class of explicit solutions can be constructed by introducing perturbations, for example poles or logarithmic branch points, into basic polynomial solutions (such as Ivantsov's dendrite), provided that all the singular points of the perturbation lie in the lower half-plane (since the mapping function f must be analytic on the upper half-plane). We consider the solutions

$$f = \omega^2 + \mathrm{i}\omega + B(t) + \sum_{k=0}^{N} d_k \ln(\omega + \alpha_k(t)), \qquad \mathrm{Im}(\alpha_k) > 0, \tag{9.1}$$

where the d_k and $\alpha_k(t)$ are complex parameters (d_k are specified constants), and $B(t)$ is real. (Similar solutions are given by Kunka, Foster & Tanveer 1997; they were constructed independently of, and concurrently with, the present work.) The d_k and α_k are subject to various constraints to ensure (9.1) is univalent on the upper-ω-plane, the most obvious of which is that $\mathrm{Im}(\alpha_k) > 0$ for all k, but we only consider the details of these constraints in the simple case $N = 1$. By far the simplest way of obtaining the evolution equations is to use the method outlined in §6, based on the fact that the singularities of the Schwarz function in the liquid domain must remain constant in position and time. Using (6.6),

$$g(z,t) = \overline{f}(\omega, t) = \omega^2 - \mathrm{i}\omega + B(t) + \sum_{k=0}^{N} \overline{d_k} \ln(\omega + \overline{\alpha_k(t)}),$$

which has branch points at $\omega = -\overline{\alpha_k}$ in the upper half-ω-plane, giving the N invariants of the flow:

$$f(-\overline{\alpha_k}) = \text{const.} = C_k, \qquad 1 \leqslant k \leqslant N,$$

whence

$$\overline{\alpha_k^2(t)} - i\overline{\alpha_k(t)} + B(t) + \sum_{r=0}^{N} d_r \log(\alpha_r(t) - \overline{\alpha_k(t)}) = C_k. \tag{9.2}$$

These are $2N$ real equations for the unknown coefficients B, α_k, so we need one more equation which comes from matching at infinity in (6.5). Since we are looking at a perturbation to the Ivantsov parabola, we want $W(z) \sim z$ at infinity. For the behaviour of $\partial g/\partial t$ at infinity we use

$$\frac{\partial g}{\partial t} = \frac{\partial \overline{f}}{\partial t} + \frac{\partial \overline{f}}{\partial \omega} \frac{\partial \omega}{\partial t},$$

where we find $\partial \omega/\partial t$ from

$$0 = \frac{\partial f}{\partial t} + \frac{\partial f}{\partial \omega} \frac{\partial \omega}{\partial t}.$$

A little algebra gives the leading-order behaviour for large $|z|$ as

$$\frac{\partial g}{\partial t} \sim \frac{1}{z^{1/2}} \left\{ \sum_{k=1}^{N} (\overline{d_k \dot{\alpha}_k} - d_k \dot{\alpha}_k) + i\dot{B} \right\};$$

matching in (6.5) then leads to

$$\dot{B} = 2\sigma + 2\text{Im}\left(\sum_{k=1}^{N} d_k \dot{\alpha}_k \right), \tag{9.3}$$

which is trivial to integrate. We remark that the 'flat interface' solution of §8 is also easily generalized in this manner, by adding on logarithmic terms to the basic mapping function.

As a simple example, consider the case $N = 1$, with $\alpha_1 = ib$, for which

$$f = \omega^2 + i\omega + B(t) + d\ln(\omega + ib(t)), \quad b > 0. \tag{9.4}$$

This is conformal on the upper half-ω-plane provided $b > 0$ and $b > d$. We may think of a 'univalency domain' in (d, b)-space, with only the region $b > 0$, $b > d$ giving univalent maps (9.4). The line $b = d > 0$ corresponds to cusped free boundary shapes, having a single $3/2$-power cusp at the point $z = f(0, t)$ on $\partial\Omega(t)$, so $f'(0, t) = 0$. In $d < 0$, as the line $b = 0^+$ is approached, free boundary shapes are generated which are basically parabolæ (with nose pointing into the liquid region), but with a parallel-sided channel of width $\pi|d|$ removed from the centre, along the axis of symmetry. Such a structure (especially when $|d| \ll 1$) may be thought of as a liquid-filled 'crack' in the solid dendrite.

In the (x, y)-plane, (9.4) gives the free boundary in parametric form as

$$x = \xi^2 + B(t) + \frac{d}{2}\ln(\xi^2 + b^2(t)),$$
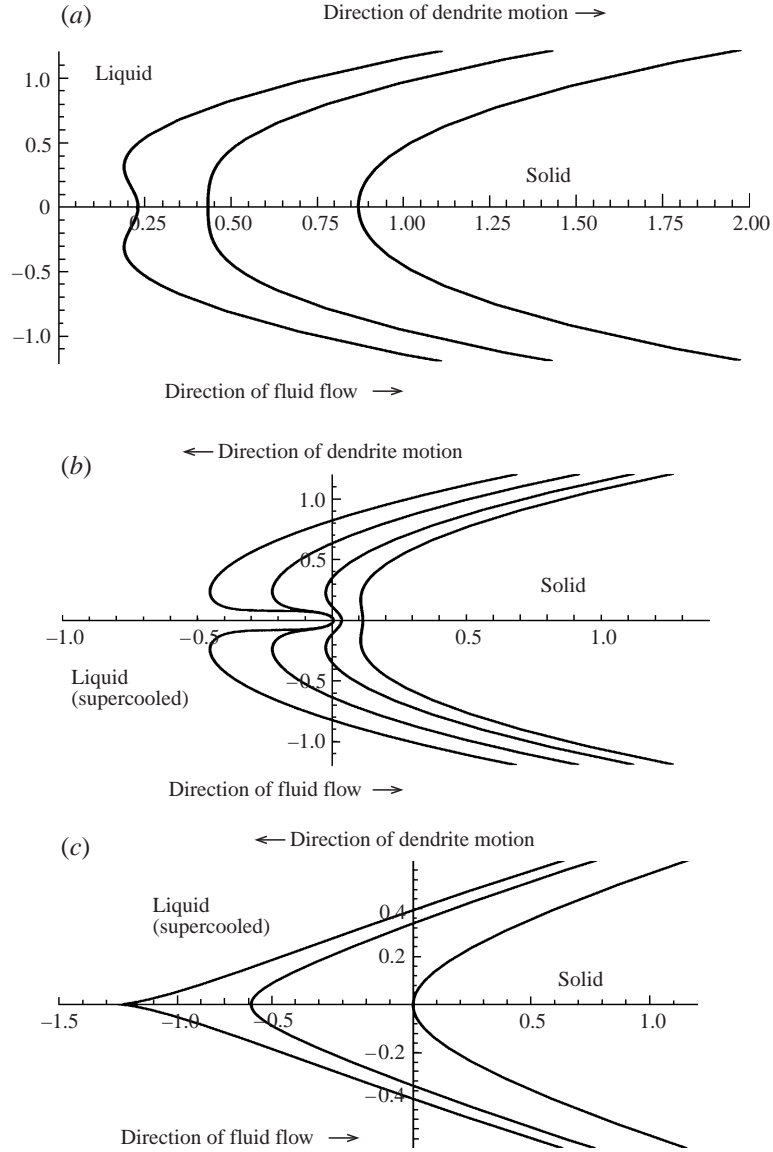
$$y = \xi + d\arctan\frac{b(t)}{\xi},$$

FIGURE 3. A typical solution of the form (9.4) in the cases of: (*a*) melting, the parameter values are $d = -0.1$, $b(0) = 0.1$, $B(0) = 0$; (*b*) crystallization, leading to a 'crack' type structure (a tip-splitting event), the parameter values are $d = -0.05$, $b(0) = 0.1$, $B(0) = 0$; (*c*) crystallization, leading to a cusped free boundary, the parameter values used are: $d = 0.5$, $b(0) = 1$, $B(0) = 0$.

for $\xi \in (-\infty, \infty)$. Evolution of the dendrite shape is determined by the branch-point dynamics as dictated by equations (9.2) and (9.3). In this simple case, solution using the P-G equation is also easy, leading to the (equivalent) system

$$B(t) = 2d(b(t) - b(0)) + 2\sigma t, \tag{9.5}$$

$$\dot{b} = \frac{b\sigma}{(b + 1/2)(b - d)}. \tag{9.6}$$

Remember that increasing time corresponds to melting, while decreasing time de-

scribes crystallization. For an initially univalent map we must have $b(0) > 0, b(0) > d$. In the melting case (9.6) then implies $\dot{b} > 0$ always, whether d is positive or negative. Hence in this case the evolution is always regular, with any initial non-uniformities in the boundary being smoothed out (figure 3*a*), and approaches the Ivantsov solution of §7 as $t \to \infty$ (this behaviour may be compared to perturbing any zero-surface-tension (ZST) Hele-Shaw travelling-wave solution, in the stable injection case).

For the case of crystallization (decreasing time) we must consider the cases $d > 0, d < 0$ separately. When $d < 0$ (9.6) gives the asymptotic behaviour of b as

$$b(t) \sim \exp\left(-\frac{2\sigma t}{d}\right), \quad t \to -\infty, \tag{9.7}$$

which consequently determines the flow pattern (the analogous asymptotic behaviour of the general solution (9.1) is also easy to obtain). The shape of the dendrite is regular at any instant of time, but as $t \to -\infty$ the 'crack-type' structure referred to above inevitably develops (figure 3*b*). This may be thought of as a 'tip-splitting' event at the dendrite tip. Such evolution may be compared with the very similar 'fingering' geometries which arise in the ZST Hele-Shaw solutions of Howison (1986), Mineev–Weinstein & Ponce–Dawson (1994) in the unstable suction case (the 'air' in the Hele-Shaw cell corresponds to the solid dendrite in our problem).

For $d > 0, b(0) > d$, analysis of (9.6) shows that b decreases towards d as t decreases, reaching d within finite time, giving cusp formation in the free boundary, at which point the solution breaks down (figure 3*c*). (In reality the appropriate regularizing surface effects would become important as such a configuration is neared; see the Conclusions below.) Note that in the reversed melting problem, such singular initial geometry would be instantly smoothed. Again, the analogy with the unstable ZST Hele-Shaw suction problem is very close, as inward-pointing cusps (relative to the liquid) are frequently obtained in such solutions.

With the more general mapping function (9.1), structures can be generated which undergo several tip-splitting events. Provided all the d_k have negative real parts, solutions to the crystallization problem can be found which exist for all time, and since the asymptotic behaviour of the time-dependent parameters is easy to determine, we can more or less choose the sequence of tip-splitting events we wish to observe, by suitably choosing the initial parameters. (Complex values of the d_k will produce non-parallel 'cracks' in the dendrite.) If some of the d_k have positive real parts, finite-time cusp formation is inevitable, but judicious choice of the initial parameter values can give solutions which first have tip-splitting events, and then break down via cusp formation (Cummings 1996).

10. Conclusions

We have demonstrated that the problem of quasi-static dendrite growth in a forced potential flow can be reformulated in terms of analytic functions. This formulation gives a method for constructing many explicit solutions, which can describe complex fingering patterns. In our example, the appearance of 'cracks' (which may be interpreted as tip-splitting events) and cusps is caused by the presence of a logarithmic branch point in the mapping function $f(\omega, t)$. Clearly, this introduction of logarithmic branch points is not a unique way of obtaining such patterns: many other combinations of poles and logarithms could be added into the basic quadratic (or linear) mapping function. In terms of the initial geometry, tip-splitting events are associated with small indentations in $\partial\Omega(0)$ relative to the solid, while cusp formation is

associated with small protruberances in $\partial\Omega(0)$. From the parallels drawn throughout this paper, it should now be clear that ZST Hele-Shaw flow and our problem of crystallization in a forced flow are closely related.

Throughout the paper we have ignored what we loosely refer to as 'regularizing surface effects' at the moving boundary, assuming them to be small. Our vagueness here is deliberate, since our model may be used to describe both ordinary two-dimensional potential flow around a frozen body (e.g. an icicle in a stream of water, or melting/freezing in a Hele-Shaw cell) and melting/freezing within a saturated porous medium. For the case of ordinary potential flow the Gibbs–Thomson condition (equating the temperature jump across the interface to the curvature of the boundary times a constant incorporating the surface tension, ordinary melting temperature and latent heat (Pamplin 1980)) is the accepted interfacial condition; however the analogous condition for the porous medium problem (with pore size within the medium assumed small relative to the size of the frozen body) remains open to debate (Dash, Haiying Fu & Wettlaufer 1995) – consider for instance the small-scale phase-change problem in the pores of the medium. Obviously, inclusion of such effects does change the dendrite shape, but we believe that the effect will be negligible except at points of high curvature of the boundary, such as may occur at crack tips, or, in the case of the cusp solutions, as the cusped state is approached. In this context we recall the assumption made earlier, that the velocity of the forced hydrodynamic flow is much greater than the velocity of crystallization. Obviously this cannot be the case as cusped configurations are approached; we also expect surface effects to become important in this situation, and for both reasons we cannot expect the model to apply in the final stages of cusp formation. Likewise, for flow in a saturated porous medium, the assumption that the characteristic size of the frozen body is much greater than the pore size is clearly violated as highly-curved geometries develop. The evolution beyond cusp formation is an even more contentious issue; it is discussed in the context of Hele-Shaw flow by Hohlov *et al.* (1994).

Returning to the analogy with the ZST Hele-Shaw problem, we note recent work by Siegel and co-workers which suggests that inclusion of even very small non-zero surface tension $\gamma \ll 1$ can have an unexpected effect on *smoothly-evolving* solutions of the ill-posed 'suction' problem (Siegel & Tanveer 1996; Seigel, Tanveer & Dai 1996) (in the sense that the solution with $\gamma \equiv 0$ is not necessarily obtained as the $\gamma \to 0+$ limit). This issue is not yet conclusively resolved however, and the relevance to our problem (particularly the porous medium case) is uncertain, since there are many other neglected small effects which may have a much greater bearing on the observed behaviour than surface tension ever does.

Nonetheless, even if we do believe our solutions capable of describing observable behaviour in both melting and solidification problems, the fact remains that we have considerable freedom to choose the parameters in the conformal maps, which naturally gives rise to questions of selection. In a similar context, we referred earlier to the non-uniqueness of the travelling-wave parabolic dendrite (both ours and Ivantsov's); only one relation exists between the tip radius and the velocity of propagation. One possible mechanism of dendritic shape selection is the influence of crystal anisotropy (Langer 1986; Kessler *et al.* 1988; Brener & Melnikov 1991). It has been conjectured on the basis of strong evidence from 'exponential asymptotics' that anisotropic surface tension breaks the Ivantsov family into a discrete set of possible shapes (Brener & Melnikov 1991) (although it is not clear whether anisotropy is the sole mechanism that can lead to a selection principle). Presumably similar ideas are needed to uniquely select the dendrite in our model, and also the appropriate tip-splitting behaviour.

Finally, it should be noted that the free boundary problem for the case of finite frozen domains may be formulated similarly; however in this case there are no explicit solutions to the Boussinesq problem, which involves finding the temperature field around a finite slit. The increased difficulty of the 'finite body' problem was mentioned in § 3. In a subsequent paper we plan to consider some numerical solutions to such problems.

REFERENCES

ALEKSANDROV, I. A. 1976 *Parametric Continuations in Theory of Univalent Functions.* Nauka, Moscow.

ANANTH, R. & GILL, W. N. 1989 Dendritic growth of an elliptical paraboloid with forced convection in the melt. *J. Fluid Mech.* **208**, 575–593.

ANANTH, R. & GILL, W. N. 1991 Self-consistent theory of dendritic growth with convection. *J. Crystal Growth* **108**, 173–189.

BENAMAR, M., BOUISSOU, P. & PELCE, P. 1988 An exact solution for the shape of a crystal growing in a forced flow. *J. Crystal Growth* **92**, 97–100.

BENSIMON, D., KADANOFF, L. P., LIANG, S. D., SHRAIMAN, B. I. & TANG, C. 1986 Viscous flows in two dimensions. *Rev. Mod. Phys.* **58**, 977–999.

BOUISSOU, P., PERRIN, B. & TABELING, P. 1989 Influence of an external flow on dendritic crystal growth. *Phys. Rev.* A **40**, 509–512.

BOUSSINESQ, M. J. 1905 *J. Math. Pure Appl.* **1**, 285.

BRATTKUS, K. & DAVIS, S. H. 1988 Flow-induced morphological instabilities: stagnation-point flows. *J. Crystal Growth* **89**, 423–427.

BRENER, E. A. & MELNIKOV, V. I. 1991 Pattern selection in two-dimensional dendritic growth. *Adv. Phys.* **40**, 53–97.

CUMMINGS, L. J. 1996 Free boundary models in viscous flow. D. Phil. Thesis, University of Oxford.

DASH, J. G., HAIYING FU, WETTLAUFER, J. S. 1995 The premelting of ice and its environmental consequences. *Rep. Prog. Phys.* **58**, 115–167.

DASH, S. K. & GILL, W. N. 1984 Forced-convection heat and momentum-transfer to dendritic structures (parabolic cylinders and paraboloids of revolution). *Intl J. Heat Mass Transfer* **27**, 1345–1356.

DAVIS, S. H. 1990 Hydrodynamic interactions in directional solidification. *J. Fluid Mech.* **212**, 241–262.

DAVIS, P. J. 1974 The Schwarz Function and its Applications. *Carus Math. Monographs* **17**, Math. Assoc. of America.

GLICKSMAN, M. E., CORIELL, S. R. & MCFADDEN, G. B. 1986 Interaction of flows with the crystal-melt interface. *Ann. Rev. Fluid. Mech.* **18**, 307–335.

GOLDSTEIN, M. E. & REID, R. I. 1978 *Proc. R. Soc. Lond.* A **364**, 45.

HOHLOV, Yu. E., HOWISON, S. D., HUNTINGFORD, C., OCKENDON, J. R. & LACEY, A. A. 1994 A model for non-smooth free boundaries in Hele-Shaw flows. *Q. J. Mech. Appl. Maths* **47**, 107–128.

HOWISON, S. D. 1986 Fingering in Hele-Shaw cells. *J. Fluid Mech.* **167**, 439–453.

HOWISON, S. D. 1988 Similarity solutions to the Stefan problem and the binary alloy problem. *IMA J. Appl. Maths* **40**, 147–161.

HOWISON, S. D. 1992 Complex variable methods in Hele-Shaw moving boundary problems. *Eur. J. Appl. Maths* **3**, 209–224.

IVANTSOV, G. P. 1947 The temperature field around a spherical, cylindrical, or point crystal growing in a cooling solution. *Dokl. Akad. Nauk. SSSR* **58**, 567 (in Russian).

KELLY, E. D. & HINCH, E. J. 1997 Numerical simulation of sink flow in the Hele-Shaw cell with small surface tension *Eur. J. Appl. Maths* **8**, 533–551.

KESSLER, D. A., KOPLIK, J. & LEVINE, H. 1988 Pattern selection in fingered growth phenomena. *Adv. Phys.* **37**, 255–339.

KOPF-SILL, A. R. & HOMSY, G. M. 1987 Narrow fingers in a Hele-Shaw cell. *Phys. Fluids* **30**, 2607–2609.

KORNEV, K. & MUKHAMADULLINA, G. 1994 Mathematical theory of freezing for flow in porous media. *Proc. R. Soc. Lond.* A **447**, 281–297.

KUNKA, M. D., FOSTER, M. R. & TANVEER, S. 1997 Dendritic crystal growth for weak undercooling. *Phys. Rev.* E **56**, 3068–3100.

LACEY, A. A. 1982 Moving boundary problems in the flow of liquid through porous media. *J. Austral. Math. Soc.* B **24**, 171–193.

LANGER, J. S. 1986 In *Direction in Condensed Matter Physics.* Memorial Volume in Honor of S. K. Ma (ed. G. Grinstein & G. Masenko), p. 165. World Scientific.

LEE, Y.-W., ANANTH, R. & GILL, W. N. 1993 Selection of a length scale in unconstrained dendritic growth with convection in the melt. *J. Crystal Growth* **132**, 226–230.

MAKSIMOV, V. A. 1965 *Izv. Acad. Nauk SSSR, Mekh.* **4**, 41.

MAKSIMOV, V. A. 1976 *Prikl. Matem. Mech.* **40**, 264.

MILLAR, R. F. 1989 An inverse moving boundary problem for Laplace's equation. In *Proc. Workshop on Inverse Problems and Imaging* (ed. G. F. Roach). London: Pitman-Longman.

MINEEV-WEINSTEIN, M. B. & PONCE-DAWSON, S. 1994 Class of nonsingular exact solutions for Laplacian pattern formation. *Phys. Rev.* E **50**, 24–27.

MULLINS, W. W. & SEKERKA, R. F. 1963 *J. Appl. Phys.* **34**, 323.

MULLINS, W. W. & SEKERKA, R. F. 1964 *J. Appl. Phys.* **35**, 444.

MUSKHELISHVILI, N. I. 1968 *Singular Integral Equations*, 3rd edn. Nauka, Moscow.

PAMPLIN, B. R. 1980 *Crystal Growth*, 2nd edn. Pergamon.

POMMERENKE, CHR. 1973 *Univalent Functions.* Vandenhoeck and Ruprecht, Göttingen.

RICHARDSON, S. 1972 Hele-Shaw flows with a free boundary produced by the injection of fluid into a narrow channel. *J. Fluid Mech.* **56**, 609–618.

SIEGEL, M. & TANVEER, S. 1996 Singular perturbation of smoothly evolving Hele-Shaw solutions. *Phys. Rev. Lett.* **76**, 419–422.

SIEGEL, M., TANVEER, S. & DAI, W. 1996 Singular effects of surface tension in evolving Hele-Shaw flows. *J. Fluid Mech.* **323**, 201–236.

WIJNGAARDEN, L. VAN 1966 *Proc. Koninkl. Nederl. Akad. Wet.* **69**, 263.

XU, J.-J. 1993 Uniformly valid asymptotic solution for steady dendrite growth in external flow. *J. Crystal Growth* **128**, 219–223.